International Journal of Advanced and Applied Sciences, 9(10) 2022, Pages: 1-10

Contents lists available at Science-Gate

International Journal of Advanced and Applied Sciences

Journal homepage: http://www.science-gate.com/IJAAS.html

Control and performance analysis of a grid-tied solar PV system

Hani Aloufi, Rabeh Abbassi *, Bassam Alhamazani, Abdullah Albaker, Mansoor Alturki, Saleh Albadran

Department of Electrical Engineering, College of Engineering, University of Ha'il, Ha'il, Saudi Arabia

ARTICLE INFO

Article history:
Received 20 February 2022
Received in revised form
21 May 2022
Accepted 19 June 2022

Keywords:
Photovoltaic systems
MPPT method
Renewable energy integration
Power quality
DC bus voltage regulation
Energy management

ABSTRACT

Considering the environmental, economic, and political context, the integration of renewable energies in electricity production has become essential. Due to its many advantages, solar photovoltaic (PV) energy is one of the most promising solutions. However, the overvoltage of the distribution line network during high power periods and the mismatch between the moments of photovoltaic production and the moments of load consumption impose limits on the integration of photovoltaic systems. This paper proposes a new method to control the integration of photovoltaic systems connected to the grid. This paper proposes a new method of control of the boost chopper for the extraction of the maximum available power (MPPT) and an adequate control system of the inverter interfacing with the grid to solve the problems related to the power quality standards. Indeed, a Modified shuffled frog leaping algorithm (MSFLA) is used to efficiently determine the values of the sliding mode controller (SMC) parameters performing the MPPT task. In addition, the power flow direction is taken into account according to the system architecture to satisfy the grid connection through the coordinated active and reactive power control of the grid side inverter. The found simulation results validate the performance of the proposed control system.

1. Introduction

Due to the increase in electricity consumption and the continuous growth of the population, the demand for energy is increasing considerably. This has led to the use of alternative energy resources that are sustainable, in addition to fossil fuels (Li et al., 2022). Globally, many countries have made huge investments to promote the use of renewable energy (RE) to cover the maximum amount of consumption. Despite this progress, the renewable energy sector is still expected to grow continuously as it still has a low participation rate compared to other fossil fuels (Tang et al., 2021; Abbassi et al., 2013). Renewable energy resources mainly flow from the earth's ecosystem such as solar, wind, geothermal energy, etc (Hosseinpour et al., 2021). As a matter of fact, the amount of natural energy available on the globe is huge, and nowadays many technologies have become mature and efficient enough for the generation of electricity (Destek and Aslan, 2020). As a matter of fact, the amount of natural energy available on the globe is huge, and nowadays many technologies have become mature and efficient enough for the generation of electricity and heat (Zhao et al., 2021). As a matter of fact, the amount of natural energy available on the globe is huge, and nowadays many technologies have become mature and efficient enough for the generation of electricity (Destek and Aslan, 2020). Renewable energy refers to the type of energy from natural and sustainable sources. The increasing importance of renewable energy stems from the environmental impact issues caused by fossil fuels which are exhaustible despite the fact that they are responsible for the generation of about 73.5% of the total energy production. In addition, due to the abundance, environmental safety, energy security, and commercial benefits, photovoltaic systems are particularly considered the most promising alternative (Hassan et al., 2020).

Knowing that the global dependence on fossil fuels will not break immediately, so integration of renewable energy systems will minimize the environmental impacts of fossil fuels and achieve the desired goals of renewable energy, strategic plans for RE integration should be conducted (Li et al., 2021). In line with the Saudi Vision 2030, a lot of work is being done to find alternatives to fossil fuels and generate electricity using renewable energy (Yin

* Corresponding Author.
Email Address: r.abbassi@uoh.edu.sa (R. Abbassi)
https://doi.org/10.21833/ijaas.2022.10.001
Corresponding author's ORCID profile:
https://orcid.org/0000-0001-8257-6721

et al., 2021). The National Renewable Energy Program (NREP) has been established to sustainably increase the share of renewable energy in Saudi Arabia's overall energy mix to 3.45 gigawatts by 2020, or about 4% of Saudi Arabia's total energy production, and 9.5 GW by 2023, or about 10% of total energy production, with a planned investment of SR 59 billion (Amran et al., 2020).

The electricity generation market based on photovoltaic generators has been growing rapidly for the past ten years. In this context, photovoltaic systems connected to the electricity distribution network are becoming increasingly important (Dutta and Chatterjee, 2017). Therefore, the quantification of the performance of the complete chain from the photovoltaic module to the power grid is essential for these applications. In particular, PV module performance is measured in terms of maximum power delivered under standard conditions (Abbassi et al., 2018a). However, from energy and financial point of view, it is the amount of energy delivered, depending on the location and implementation of the modules, that matters. This is why research on methods for predicting the behavior of solar modules under real sunlight conditions, and in terms of energy produced and/or average yield under real operating conditions, is particularly important. Numerous studies on the electrical behavior of PV modules have highlighted several factors that have a significant influence on the efficiency of the conversion of radiation into electricity: The level of incident illumination on the modules, the spectrum of this radiation, and the operating temperature of the photovoltaic cells (Abbassi et al., 2020; 2018c). In addition, extracting the maximum available power through a maximum power point tracking (MPPT) algorithm is an essential task to improve the efficiency of the photovoltaic conversion chain.

In addition, the investigation of different problems related to photovoltaic applications has been the subject of various works. The common objective was to propose some solutions for the control of interfacing converters that may be present in a PV system connected to the grid. Indeed, the PV generator is subject to meteorological uncertainties (Hamidi et al., 2020; Hassan et al., 2020). To overcome these intermittent effects, the DC/DC boost converter must be controlled via an MPPT algorithm in order to eliminate the multiplicity of local power maxima that can cause a considerable drop in production (Latifi et al., 2021; Mohammadinodoushan et al., 2021). Such algorithms dedicated to finding a point of maximum power in cases where the illumination is non-uniform are necessary. On the other hand, minimizing the adverse effects caused by the interactions between the grid impedance and the associated power electronics, on behalf of the inverter, needs to be addressed to overcome the stability issues related to disturbances generated by the end users connected to the AC grid that can cause the overall instability of the system (Abbassi et al., 2018a). Similarly, the interaction of the power electronics with the passive RL, LC, or LCL interconnect filters, which causes stable or unstable limit cycles, must be addressed to ensure high quality of power via grid side inverter control interfacing with the grid (Abbassi et al., 2015).

The rapid growth in the use of solar energy has provided consumers with a more secure supply while reducing the risk to the environment. However, the unpredictable nature of these sources requires that supply and/or grid regulations should be established for optimal system operation to overcome the major drawback of fluctuations in such a source regardless of the consumption profile (Saidi et al., 2016). However, these conversion systems are becoming more and more affordable and their important contribution to sustainable energy use still requires considerable development of storage technologies. This will open up a new field of application, especially due to the growth of electricity production from renewable energies, as well as decentralized production.

Energy storage is becoming recognized as a key component of the modern energy supply chain due to its ability to improve grid stability, promote the penetration of renewable energy resources, increase the efficiency of energy systems, rationalize the use of exhaustible resources and reduce negative environmental impacts (Abbassi et al., 2019). In the literature, different energy storage technologies with different levels of technological maturity have already been proposed. Among them, a large family has already been proven in various commercialized applications (Abbassi et al., 2018b). Most of the research work on energy storage systems has attempted to provide a synthesis that offers a detailed analysis of the benefits of these systems and their actual performance for each application field.

2. Modelling of the system

The conversion of PV energy into alternative electrical energy suitable for the grid is essentially based on the following constituent elements: The PV module, the DC/DC converter controlled by the MPPT controller to bring the operating point of the PV system back to the maximum power point (MPP) and the grid side inverter which converts DC electrical energy into AC energy (Abbassi et al., 2019). In turn, the inverter is responsible for performing the following tasks:

- Adjust the AC output voltage to the maximum admissible value for the network.
- Ensure perfect synchronization with the network.
- Minimize phase shift.
- Reduce the rate of harmonic frequencies in order to have an output signal close to the maximum of a sine wave.
- Reduce electromagnetic interference.
- Guarantee the high efficiency of the power transferred to the grid.

The structure adopted in this paper is shown in Fig. 1. It shows that the PV generator is connected to the network via a DC/DC boost converter, a DC bus, a three phase inverter, and a low pass filter.

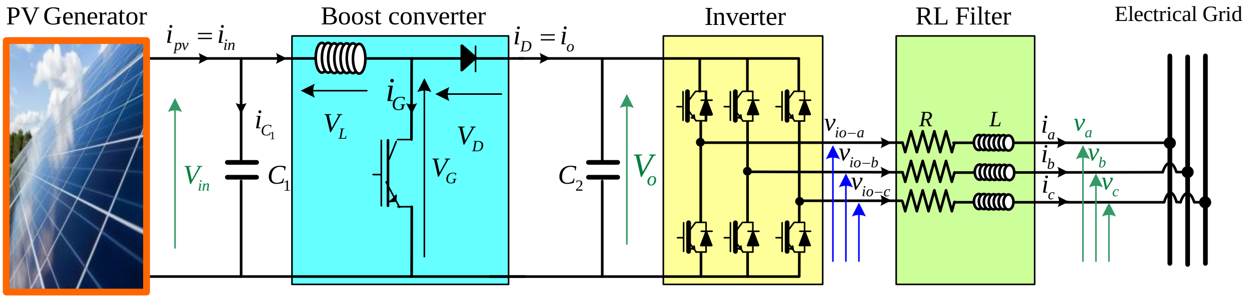

Fig. 1: Grid-connected PV system

2.1. Modelling of the PVG

The two-diode electric model of the real PV cell is the one shown in Fig. 2 (Abbassi et al., 2018c), it contains:

- A source of photo-generated current Iph.
- Rs is a series resistance that simulates the impedance of electrodes and materials and volume resistivity.
- Rp is a shunt resistance linked to edge effects and volume recombinations.

The slopes of the current-voltage curve at points Voc and Isc represent the inverse of the series resistance (1/Rs) and the inverse of the shunt resistance (1/Rp), respectively.

- Diodes D1 and D2.

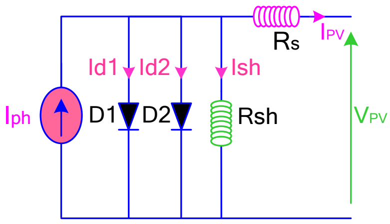

Fig. 2: Equivalent circuit of the practical double-diode model

Taking into account the influence of meteorological conditions, materialized by the difference between the values of the ambient temperature and irradiation (T and G) and those of the temperature and irradiation of STC conditions (T_n and G_n), the current generated is (Abbassi et al., 2018a):

$$I_{PV}(G,T) = \frac{G}{G_n}[I_{scn} + K_i(T - T_n)] - \frac{I_{scn}+K_i(T-T_n)}{exp\left(\frac{V_{ocn}+I_{scn}(T-T_n)}{nN_sk_BT/q}\right)-1} \cdot \left[exp\left(\frac{v_{PV}}{nN_sk_BT/q}\right) - 1\right] \quad (1)$$

where, q is the charge of an electron, N_s is the number of PV cells in series, k_B is the Boltzmann constant. V_{ocn} is the open circuit voltage, I_{scn} is the cell's short circuit current at STC and k_v and k_i are, respectively, their variation coefficients, n is the diode ideality factor.

In order to calculate the current generated by a PV generator composed of N_p panels connected in parallel and N_{ss} panels connected in series, Eq. 1 becomes:

$$I_{PV}(\mathrm{G,T}) = \frac{\mathrm{G}}{G_n} N_p[I_{scn} + K_i(T - T_n)] - \frac{(I_{scn}+K_i(T-T_n))N_p}{\exp\left(\frac{(V_{ocn}+I_{scn}(T-T_n))N_{SS}}{nN_sN_{ss}k_BT/q}\right)-1} \cdot \left[\exp\left(\frac{V_{PV}}{nN_sN_{ss}k_BT/q}\right) - 1\right] \quad (2)$$

The total power is:

$$P_{PV}(\mathrm{G,T}) = I_{PV}(\mathrm{G,T}).V_{PV}(\mathrm{G,T}) \quad (3)$$

At this stage, the determination of the voltage of the maximum power point guarantees that the adjustment of the DC/DC chopper duty cycle is suitably done.

2.2. MPPT control

The MPPT controller is generally designed to deal with the constraints caused by climate change (Hamidi et al., 2020). The performance of this controller depends on how quickly to reach the point of maximum power, how to oscillate around that point, and how robust this controller is in the face of abrupt atmospheric changes such as partial shading. Since the MPPT technique is the focus of various works, the present work has given it paramount importance to improving the dynamic performance of the PV system. The criteria for judging performance are primarily related to the ability to rapidly pursue the global power point (GMPP) in the presence of other local maximums during partial shading (Abbassi et al., 2020).

In this work, the MPPT technique used is the one called Modified shuffled frog leaping algorithm (MSFLA)-Sliding Mode Controller (SMC) (Mohammadinodoushan et al., 2021). The flowchart of MSFLA is shown in Fig. 3. The MSFLA is combined with the SMC theory to perform the MPPT task. In fact, the MSFLA allows effectively determining the values of the SMC parameters.

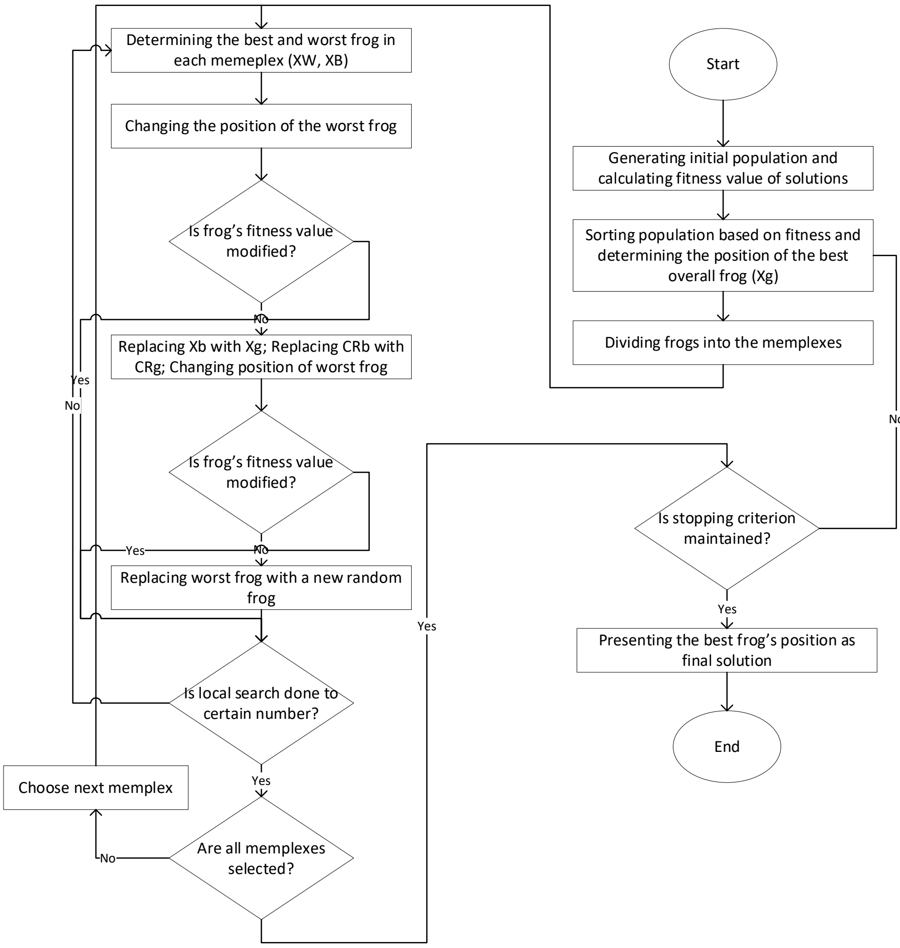

Fig. 3: The MSLFA flowchart (Mohammadinodoushan et al., 2021)

3. DC-AC control strategy

3.1. Internal and external control loops

The DC/AC is responsible for the interface between the DC bus and the three-phase AC network. This VSI type converter must also take care of the control of active and reactive power by acting on the voltages and currents injected at the PCC point. This type of control is necessarily ensured by internal loops for the currents and external loops for the voltages since the dynamics of the currents are faster than that of the voltages (Abbassi et al., 2019). Fig. 4 illustrates the developed control scheme.

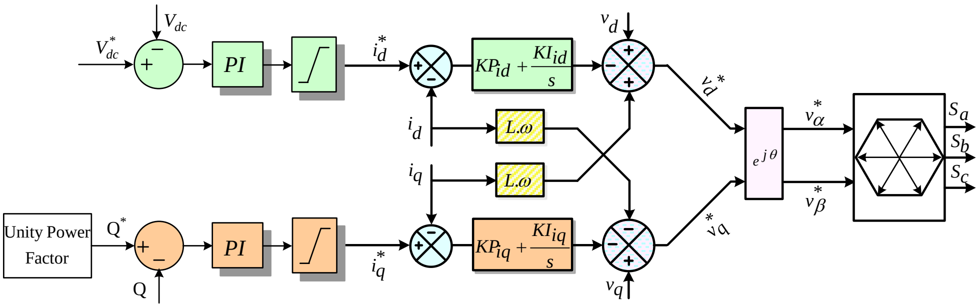

Fig. 4: Block diagram of the DC-AC converter PI control

The control of currents and voltages can be provided according to state variables or by means of a cascade structure thanks to the ability of the converter to be used as a controlled current source or as a controlled voltage source (Dutta and Chatterjee, 2017). The double loop control is the most used. The control is done by the dynamic response of the internal current loop controller which is fast.

The dynamic response of the external voltage loop controller is slower and is reserved for different control purposes and to produce the internal reference signal. In what follows, the control strategy of the inverter will be discussed. In the three-phase diagram of the inverter presented in Fig. 1, the grid voltages are: $v_a(t)$, $v_b(t)$and $v_c(t)$, the currents injected into the grid are $i_a(t)$, $i_b(t)$and $i_c(t)$ and the voltages at the inverter output are $v_{io-a}(t)$,

$v_{io-b}(t)$and $v_{io-c}(t)$. The resistance and the inductance of the filter are indicated, respectively, by R&L (Abbassi et al., 2018b).

Based on the fact that in grid-connected mode, the frequency and voltage at the interconnection point are imposed by the electrical grid, we express the following grid voltages:

$$v_a(t) = V_m.sin(w.t)$$
$$v_b(t) = V_m.sin\left(w.t - \frac{2\cdot\Pi}{3}\right) \quad (4)$$
$$v_c(t) = V_m.sin\left(w.t + \frac{2\cdot\Pi}{3}\right)$$

By applying Kirchhoff's law of voltages, we obtain the following differential equations for the three phases.

$$v_{io-a}(t) - v_a(t) - R.i_a(t) - L.\frac{d}{dt}i_a(t) = 0$$
$$v_{io-b}(t) - v_b(t) - R.i_b(t) - L.\frac{d}{dt}i_b(t) = 0 \quad (5)$$
$$v_{io-c}(t) - v_c(t) - R.i_c(t) - L.\frac{d}{dt}i_c(t) = 0$$

To ensure regulation of the currents and voltages at the output of the inverter, the expressions for the voltages in the Park synchronous reference frame must be set as follows:

$$V_d(t) = \sqrt{\frac{2}{3}}\cdot\left(\cos(\omega\cdot t).v_a(t) + \cos(\omega\cdot t - \frac{2\cdot\Pi}{3}).v_b(t) + \cos(\omega\cdot t + \frac{2\cdot\Pi}{3}).v_c(t)\right)$$
$$V_q(t) = \sqrt{\frac{2}{3}}\cdot\left(-\sin(\omega\cdot t).v_a(t) - \sin(\omega\cdot t - \frac{2\cdot\Pi}{3}).v_b(t) - \sin(\omega\cdot t + \frac{2\cdot\Pi}{3}).v_c(t)\right) \quad (6)$$
$$V_o(t) = \sqrt{\frac{2}{3}}\cdot\sqrt{\frac{1}{2}}\left(v_a(t) + v_b(t) + v_c(t)\right)$$

Here, the use of the Park transform allows us to obtain constant quantities in the rotating reference frame (d, q) from sinusoidal three-phase quantities. Indeed, we have used the following transformation matrix for voltages and currents:

$$\begin{bmatrix} V_d(t) \\ V_q(t) \\ V_0(t) \end{bmatrix} = \sqrt{\frac{2}{3}}\cdot\begin{bmatrix} \cos(\omega.t) & \cos(\omega.t - \frac{2\pi}{3}) & \cos(\omega.t + \frac{2\pi}{3}) \\ -\sin(\omega.t) & -\sin(\omega.t - \frac{2\pi}{3}) & -\sin(\omega.t + \frac{2\pi}{3}) \\ \frac{1}{\sqrt{2}} & \frac{1}{\sqrt{2}} & \frac{1}{\sqrt{2}} \end{bmatrix}\begin{bmatrix} v_a(t) \\ v_b(t) \\ v_c(t) \end{bmatrix} \quad (7)$$

In a later phase, the Concordia transform which allows having the quantities in the stationary reference frame is used. This transformation corresponds to the Park matrix with a zero angle. The reference voltages of axes (d, q) are then rewritten in the stationary reference frame of Concordia with the following relationship (Abbassi et al., 2018b):

$$V^*_{i\circ-\alpha}(t) + j.V^*_{i\circ-\beta}(t)) = e^{j.\theta}.(V^*_{i\circ-d}(t) + j.V^*_{i\circ-q}(t)) \quad (8)$$

Similarly, the transformation of the voltages vector at the output of the inverter $v_{i\circ-a,b,c}(t)$ and the currents vector $i_{a,b,c}(t)$ in Park's rotating reference frame allows us to rewrite the previous relationship that becomes:

$$V_{-i\circ-dq}(t) - V_{-i\circ-dq}(t) - R.I_{-dq}(t) - L.\frac{d}{dt}I_{-dq}(t) - j.\omega.L.\frac{d}{dt}I_{-dq}(t) = 0 \quad (9)$$

In an attempt to generate the $V_{i\circ-d}$ and $V_{i\circ-q}$ components of the inverter output voltages, a space vector PWM control block uses the reference signals of these voltages in the stationary reference frame (α, β). The reference signals of the voltages are obtained according to Fig. 4.

4. Results and discussion

For the first simulations presented by Figs. 5, and 6, the I-V and P-V characteristics are shown respectively. They were done under ideal conditions commonly known as standard test conditions. These ideal conditions refer to specific situations where the illuminance is 1000 w/m² and the temperature is 25°C.

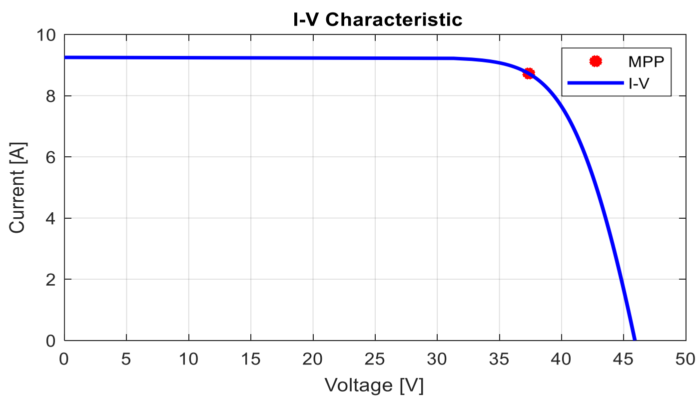

Fig. 5: I-V characteristic in STC

The power curve of a GPV passes through a particular maximum power point (MPP) which depends on the changes in the weather conditions. Thus, the DC-DC converter is integrated to allow the modification of the panel's operating point thanks to the MPPT control.

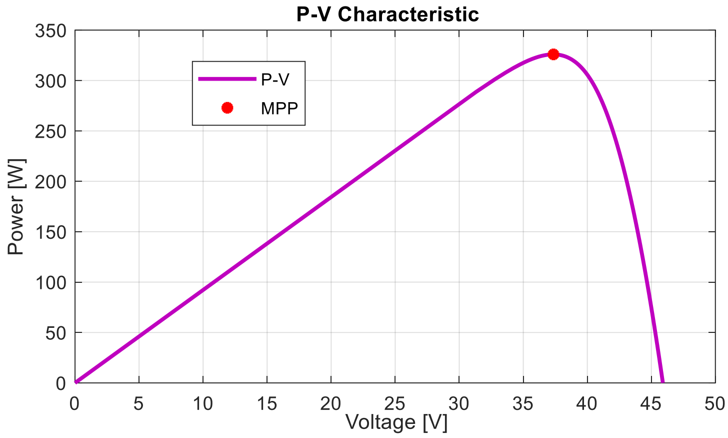

Fig. 6: P-V characteristic in STC

The effect of the irradiance variation on the I-V characteristic is shown in Fig. 7. It is clear that the current varies strongly with irradiance variation while the voltage varies weakly with such variation. This is justified because the short circuit current is a linear function of the irradiance while the open circuit voltage is a logarithmic function.

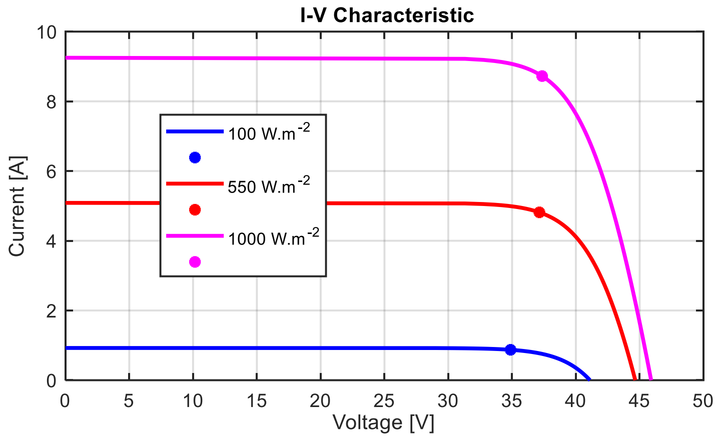

Fig. 7: Effect of the irradiance variation on the I-V characteristics

The effect of illumination variation on the P-V characteristic is shown in Fig. 8. It is clear that as proportional to the current, the power is clearly sensitive to the variation of the illumination.

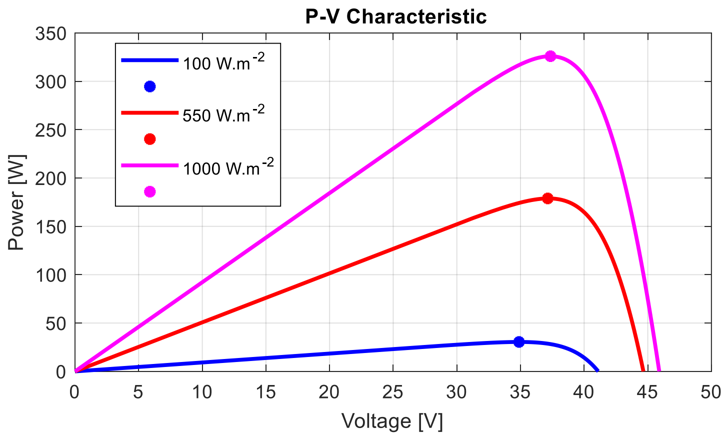

Fig. 8: Effect of the irradiance variation on the P-V characteristics

By examining the effect of temperature on the I-V characteristic and unlike the proportionality of the short circuit current to the incident solar radiation, the open circuit voltage increases rapidly as the temperature decreases (Fig. 9).

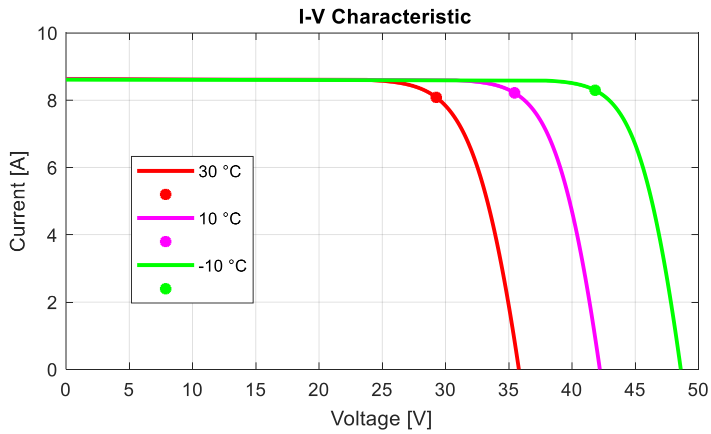

Fig. 9: I-V characteristic in STC

It is clear from the previous simulations that the power output of the PV generator depends directly on solar irradiance and temperature. Indeed, with the change in the weather conditions, the point of maximum power (MPP) changes clearly. Fig. 10 shows the P-V characteristic in STC.

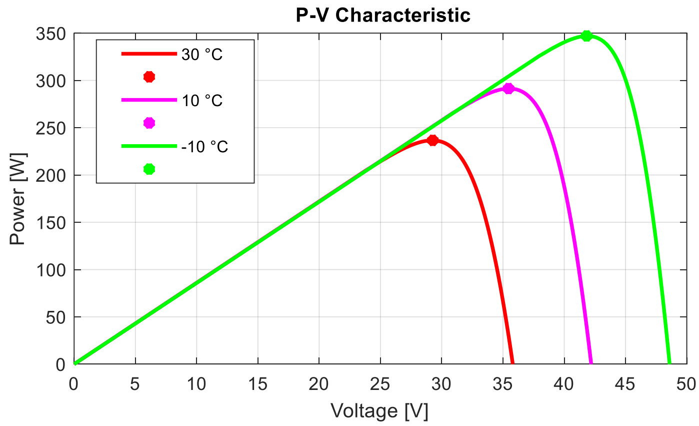

Fig. 10: P-V characteristic in STC

Therefore, the DC/DC converter is integrated to ensure the maximum power available regardless of the variable and unpredictable weather conditions.

In the following, the study focuses on the performance evaluation of the photovoltaic system connected to a balanced three-phase grid through a DC bus. In particular, two levels of control of the power electronics converters have been developed under the Matlab/Simulink environment to benefit the most from this type of fluctuating and unpredictable source and to push its efficiency for grid-connected applications. In fact, the first level of study has been related to the control of the DC-DC chopper which is responsible for the extraction of the maximum of the available power, while the second level has been given to the control of the DC-AC inverter which interfaces with the connection network and which takes care of the control of the electric quantities exchanged with the power network and of the power quality.

The PV system is formed by a PV generator constituted by the association of 60 panels of type GT PV 216 poly with a peak power of 216 W. For the simulations performed, the insolation profile is shown in Fig. 11. Abrupt variations of this parameter are assumed to judge the performance of the adopted control systems.

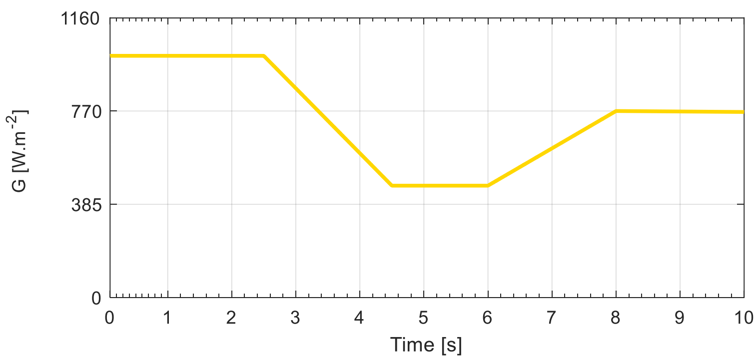

Fig. 11: Irradiance variations

As a result of the MPPT control of the DC-DC boost converter and the control of the DC-AC converter on the grid side, we have simulated the temporal evolutions of the generated electrical quantities. Initially, the voltages at the grid connection point are shown in Fig. 12.

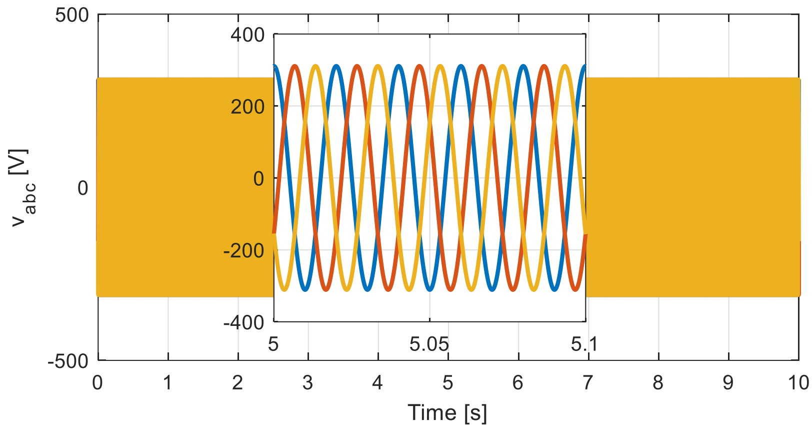

Fig. 12: Grid voltages

As shown in Fig. 13, the currents generated by the inverter vary depending on the variation of the irradiance. In fact, the amplitude of the currents shows the same trend as that of the solar irradiance.

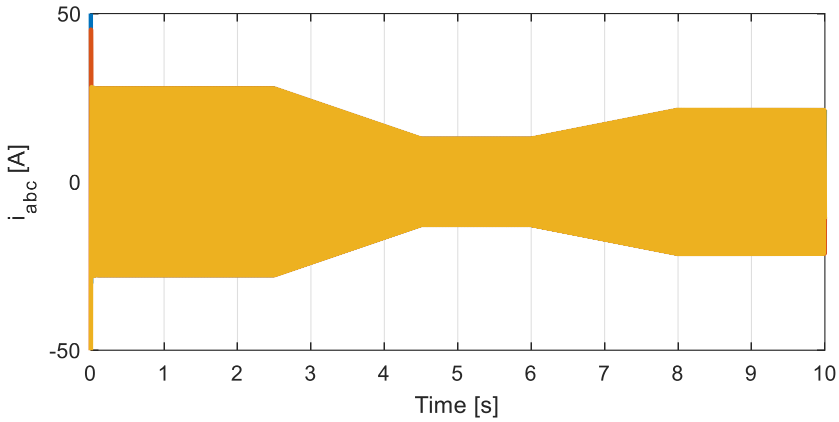

Fig. 13: Grid side currents

The zooms made show more clearly that the generated currents are perfectly balanced. Moreover, the amplitude of the currents reflects the power generated by PV. Fig. 14 shows zooms of the grid currents.

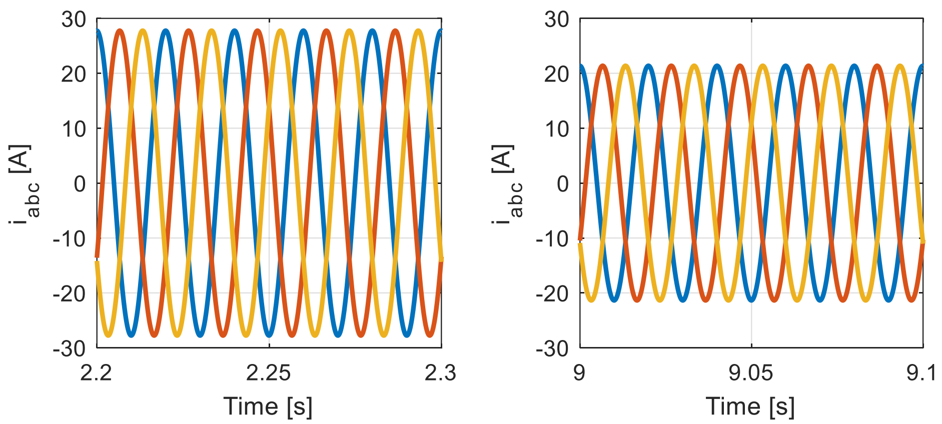

Fig. 14: Zooms of the grid currents

Regarding the active and reactive powers injected into the electrical grid, their curves are shown in Figs. 15a, and 15b, respectively. It is shown that the active power varies in dependence of the irradiance and the power of the PV generator as long as the reactive power is zero.

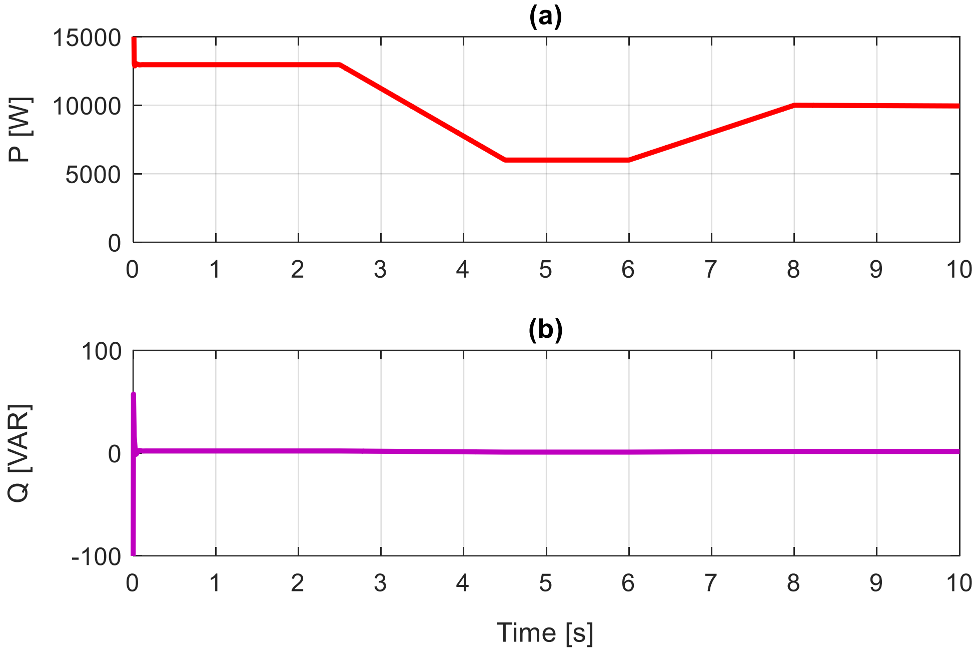

Fig. 15: Grid (a) active and (b) reactive powers

It is shown in Fig. 15 that the active power varies in dependence on the irradiance and the power of the PV generator as long as the reactive power is zero.

5. Conclusion

The presented work focused on the modeling and simulations of the components of a photovoltaic system connected to the electrical grid. In particular, the control of the step-up DC/DC converter has been highlighted by the MPPT technique. In addition, the control of the DC/AC inverter responsible for the connection to the electrical grid was provided by the SVM vector modulation technique. The analysis of the simulation results allowed us to evaluate the influence of the external weather conditions on the operation of the solar photovoltaic system and its control aspects. Also, insight into the problems and difficulties related to grid-connected photovoltaic systems has been investigated. Future horizons can be opened by the combination of the PV system with other renewable sources such as wind systems. Moreover, the integration of a storage system can also be a reliable solution to the intermittency of PV energy sources.

Acknowledgment

This research has been funded by Scientific Research Deanship at the University of Ha'il–Saudi Arabia through project number GR-22 078.

Compliance with ethical standards

Conflict of interest

The author(s) declared no potential conflicts of interest with respect to the research, authorship, and/or publication of this article.

References

Abbassi A, Abbassi R, Heidari AA, Oliva D, Chen H, Habib A, and Wang M (2020). Parameters identification of photovoltaic cell models using enhanced exploratory salp chains-based approach. Energy, 198: 117333. https://doi.org/10.1016/j.energy.2020.117333

Abbassi R, Abbassi A, Jemli M, and Chebbi S (2018a). Identification of unknown parameters of solar cell models: A comprehensive overview of available approaches. Renewable and Sustainable Energy Reviews, 90: 453-474. https://doi.org/10.1016/j.rser.2018.03.011

Abbassi R, Abbassi A, Marrouchi S, Saidi S, and Chebbi S (2018b). Power conditioning and integration improvement for wind-PV-batteries hybrid system to faulty power systems. In the 15th International Multi-Conference on Systems, Signals and Devices, IEEE, Yasmine Hammamet, Tunisia: 1122-1127. https://doi.org/10.1109/SSD.2018.8570464

Abbassi R, Boudjemline A, Abbassi A, Torchani A, Gasmi H, and Guesmi T (2018c). A numerical-analytical hybrid approach for the identification of SDM solar cell unknown parameters. Engineering Technology and Applied Science Research, 8(3): 2907-2913. https://doi.org/10.48084/etasr.2027

Abbassi R, Hammami M, and Chebbi S (2013). Improvement of the integration of a grid-connected wind-photovoltaic hybrid system. In the International Conference on Electrical Engineering and Software Applications, IEEE, Hammamet, Tunisia: 1-5. https://doi.org/10.1109/ICEESA.2013.6578357

Abbassi R, Marrouchi S, Saidi S, Abbassi A, and Chebbi S (2019). Optimal energy management strategy and novel control approach for DPGSs under unbalanced grid faults. Journal of Circuits, Systems and Computers, 28(4): 1950-1957. https://doi.org/10.1142/S0218126619500579

Abbassi R, Saïdi S, Marrouchi S, and Chebbi S (2015). Novel flexible algorithm for the operation of renewable source grid interface VSCs under unbalanced voltage sags. In the IEEE 15th International Conference on Environment and Electrical Engineering, IEEE, Rome, Italy: 1414-1419. https://doi.org/10.1109/EEEIC.2015.7165377

Amran YA, Amran YM, Alyousef R, and Alabduljabbar H (2020). Renewable and sustainable energy production in Saudi Arabia according to Saudi Vision 2030; Current status and future prospects. Journal of Cleaner Production, 247: 119602. https://doi.org/10.1016/j.jclepro.2019.119602

Destek MA and Aslan A (2020). Disaggregated renewable energy consumption and environmental pollution nexus in G-7 countries. Renewable Energy, 151: 1298-1306. https://doi.org/10.1016/j.renene.2019.11.138

Dutta S and Chatterjee K (2017). A buck and boost based grid connected PV inverter maximizing power yield from two PV arrays in mismatched environmental conditions. IEEE Transactions on Industrial Electronics, 65(7): 5561-5571. https://doi.org/10.1109/TIE.2017.2774768

Hamidi F, Olteanu SC, Popescu D, Jerbi H, Dincă I, Ben Aoun S, and Abbassi R (2020). Model based optimisation algorithm for maximum power point tracking in photovoltaic panels. Energies, 13(18): 4798. https://doi.org/10.3390/en13184798

Hassan TU, Abbassi R, Jerbi H, Mehmood K, Tahir MF, Cheema KM, and Khan IA (2020). A novel algorithm for MPPT of an isolated PV system using push pull converter with fuzzy logic controller. Energies, 13(15): 4007. https://doi.org/10.3390/en13154007

Hosseinpour M, Soltani M, and Nathwani J (2021). Renewable energy integration with hot compressed water in heavy oil upgrading: A practice toward sustainability. Journal of Cleaner Production, 334: 130268. https://doi.org/10.1016/j.jclepro.2021.130268

Latifi M, Abbassi R, Jerbi H, and Ohshima K (2021). Improved krill herd algorithm based sliding mode MPPT controller for variable step size P&O method in PV system under simultaneous change of irradiance and temperature. Journal of the Franklin Institute, 358(7): 3491-3511. https://doi.org/10.1016/j.jfranklin.2021.02.021

Li J, Luo Y, and Wei S (2022). Long-term electricity consumption forecasting method based on system dynamics under the carbon-neutral target. Energy, 244: 122572. https://doi.org/10.1016/j.energy.2021.122572

Li N, Su Z, Jerbi H, Abbassi R, Latifi M, and Furukawa N (2021). Energy management and optimized operation of renewable sources and electric vehicles based on microgrid using hybrid gravitational search and pattern search algorithm. Sustainable Cities and Society, 75: 103279. https://doi.org/10.1016/j.scs.2021.103279

Mohammadinodoushan M, Abbassi R, Jerbi H, Ahmed FW, and Rezvani A (2021). A new MPPT design using variable step size perturb and observe method for PV system under partially shaded conditions by modified shuffled frog leaping algorithm-SMC controller. Sustainable Energy Technologies and Assessments, 45: 101056. https://doi.org/10.1016/j.seta.2021.101056

Saidi S, Abbassi R, and Chebbi S (2016). Quality improvement of shunt active power filter with direct instantaneous power estimator based on virtual flux. International Journal of Control, Automation and Systems, 14(5): 1309-1321. https://doi.org/10.1007/s12555-014-0264-4

Tang S, Jiang M, Abbassi R, and Jerbi H (2021). A cost-oriented resource scheduling of a solar-powered microgrid by using the hybrid crow and pattern search algorithm. Journal of Cleaner Production, 313: 127853. https://doi.org/10.1016/j.jclepro.2021.127853

Yin N, Abbassi R, Jerbi H, Rezvani A, and Müller M (2021). A day-ahead joint energy management and battery sizing framework based on θ-modified krill herd algorithm for a renewable energy-integrated microgrid. Journal of Cleaner Production, 282: 124435. https://doi.org/10.1016/j.jclepro.2020.124435

Zhao L, Jerbi H, Abbassi R, Liu B, Latifi M, and Nakamura H (2021). Sizing renewable energy systems with energy storage systems based microgrids for cost minimization using hybrid shuffled frog-leaping and pattern search algorithm. Sustainable Cities and Society, 73: 103124. https://doi.org/10.1016/j.scs.2021.103124